maximum power transfer from the feed to the antenna can be achieved through a simple coplanar waveguide matching network on the ground plane of the antenna.

## IV. Conclusion

A printed star antenna with five feeding points is proposed for the generation of doughnut and tilted patterns. When fed at the centre, the antenna radiates a doughnut pattern with a directivity of about 5.1 dBi, comparable to that of the top-loaded monopole over a ground plane. If it is excited at any of its four corners, the antenna generates a tilted beam with a directivity varying between 3.4 dBi and 7.9 dBi depending on the flare angle of the star. Also, by varying the flare angle, a beam tilt variation from $42^\circ$ to $62^\circ$ can be achieved in the corner fed configuration. When the five feeding points are excited individually a large portion of space in front of the antenna can be scanned by virtue of five distinct patterns, all of which have the polarization dominance in the $E_\theta$ direction. It should be mentioned that the feed network envisaged for the antenna can make use of the coplanar waveguide. The coplanar waveguide can be readily etched on the ground plane of the antenna, providing a medium for the implementation of the necessary impedance matching circuit for the antenna.

## References


[1] A. Mehta, D. Mirshekar-Syahkal, and H. Nakano, "Beam adaptive single arm rectangular spiral antenna with switches," in *Proc. IEE Microw. Antennas Propag.*, Feb. 2006, vol. 153, pp. 13–18.

[2] C. Won, M.-J. Lee, G. P. Li, and F. De Flaviis, "Reconfigurable beam-scan single-arm spiral antenna with integrated MEMS switches," *IEEE Trans. Antennas Propag.*, vol. 54, no. 2, pp. 455–463, Feb. 2006.

[3] G. H. Huff and J. T. Bernhard, "Integration of packaged RF MEMS switches with radiation pattern reconfigurable square spiral microstrip antennas," *IEEE Trans. Antennas Propag.*, vol. 54, no. 2, pp. 464–469, Feb. 2006.

[4] A. Mehta and D. Mirshekar-Syahkal, "Pattern steerable square loop antenna," in *IEE Electron. Lett. (IET)*, Apr. 26, 2007, pp. 491–493.

[5] A. Mehta, D. Mirshekar, and H. Nakano, "A novel star patch antenna for beam steering applications," in *Proc. IEEE APS Conf.*, HI, Jun. 10–15, 2007, pp. 5857–5860.

[6] CST GmbH. Darmstadt, Germany.

[7] SATIMO. Courtaboeuf, France.

[8] S. Honda, M. Ito, H. Seki, and Y. Jinbo, "A disc monopole antenna with 1:8 impedance bandwidth and omni-directional radiation pattern," in *Proc. Int Symp. Antennas Propag.*, Sapporo, Japan, 1992, pp. 1145–1148.

[9] N. P. Agrawall, G. Kumar, and K. P. Ray, "Wide-band planar monopoles," *IEEE Trans. Antennas Propag.*, vol. 46, pp. 294–295, Feb. 1998.

[10] K. L. Lau and K. M. Luk, "A wide-band monopolar wire-patch antenna for indoor base station applications," *IEEE Antennas Wireless Propag. Lett.*, vol. 4, pp. 155–157, 2005.

[11] K. W. Chan, K. F. Tong, and K. Man Luk, "Wideband circular patch antenna operated at TM01 mode," *Electron. Lett.*, vol. 35, no. 24, pp. 2070–2071, Nov. 1999.

[12] V. G. Posadas, D. S. Vargas, E. R. Iglesias, J. L. V. Roy, and C. M. Pascual, "Approximate analysis of short circuited ring patch antenna working at TM01 mode," *IEEE Trans. Antennas Propag.*, vol. 54, pp. 1875–1879, Jun. 2006.

[13] J. S. Row and S.-H. Chen, "Wideband monopolar square-ring patch antenna," *IEEE Trans. Antennas Propag.*, vol. 54, pp. 1335–1339, Apr. 2006.

[14] M. R. Kamarudin, P. S. Hall, F. Colombel, and M. Himdi, "Switchable disk-loaded monopole antenna array with CPW feeding system," in *Proc. IEEE Antenna and Propag. Symp.*, Jul. 9–14, 2006, pp. 2313–2316.

[15] X. Liang, S. Zhong, and W. Wang, "Tapered CPW-fed printed monopole antenna," *Wiley Microw. Opt. Tech. Lett.*, vol. 48, no. 7, pp. 1411–1413, Jul. 2006.

[16] H. Kanaya, R. Nabeshima, R. Pokharel, K. Yoshida, M. Tsujii, and R. Iino, "Development of an electrically small one-sided directional antenna with matching circuit," in *IEEE Radio and Wireless Symp. (RWS 2008)*, Orlando, FL, Jan. 22–24, 2008, pp. 739–742.

[17] J. Villanen, C. Icheln, and P. Vainikainen, "Mobile broadband antennas," presented at the Proc. XXVIIth URSIGA Conf., New Delhi, India, Oct. 2005.


# Design of a Circularly Polarized Tag Antenna for Increased Reading Range

Chihyun Cho, Ikmo Park, and Hosung Choo

***Abstract*—We introduce a novel circularly polarized tag antenna, consisting of a truncated patch, a shorting plate, and a ground plane, to increase the reading range while remaining in compliance with EIRP regulations. The reading range of the proposed tag is twice that of linearly polarized tags, due to the decreased polarization mismatch between the reader and tag antennas. An additional parasitic patch is loaded onto the structure to boost the reading range in the UHF RFID band. As a result, an average reading range of 8 m is achieved between 860 MHz and 960 MHz, compared to a range of about 3 m with conventional dipole tags.**

***Index Terms*—Antenna, circular polarization, radio frequency identification (RFID, tag.**

## I. Introduction

Passive ultrahigh frequency (UHF) radio frequency identification (RFID) systems have been widely used in many applications, such as supply chains, highway tollbooths, and security systems [1]–[4]. To increase the reading range of passive RFID systems, readers and tag chips with highly sensitive signal detection capabilities are required, adding considerably to the manufacturing costs. The reading range can also be increased by boosting the transmission power of the reader, but the amount of power is limited by the local equivalent isotropic radiated power (EIRP) regulations of each country [5]. Another way to augment the reading range is to increase the polarization efficiency between the reader and tag antennas. Most RFID systems employ reader antennas with circular polarization (CP) to consistently detect dipole-type tags. The resulting polarization mismatch between the tag and reader antennas reduces the maximum attainable reading range of the system. For practical application in a commercial RFID system, the CP tag antenna should have a broad matching bandwidth, a CP bandwidth from 860 to 960 MHz, and a simple planar structure.

In this communication, we introduce a novel CP tag antenna that exhibits broad impedance matching and CP bandwidth, and has a simple planar structure. The proposed tag antenna consists of a single radiating patch, a shorting plate, and a ground plane. For impedance matching with commercial tag chips, the feed line is added between the patch and the ground plane, resulting in the attainment of a broad bandwidth entirely covering the UHF RFID band. A high axial ratio (AR) close to 1 is obtained near 910 MHz by truncating the edge of the patch. By studying the relationship between the reading range and AR, we found that the reading range is predominantly determined by the RHCP gain of the tag antenna. Accordingly, we modified the antenna structure by loading an additional parasitic patch on top of the main radiator to boost the RHCP gain. This resulted in a reading range of more than 7.5 m over a broad bandwidth, whereas commercial dipole-type tags have a reading range of about 3 m.

Manuscript received September 12, 2008; revised February 27, 2009. First published July 28, 2009; current version published October 07, 2009.

C. Cho is with the Institute of advanced technologies, Samsung Thales, Yongin, Korea

I. Park is with the Department of Electrical and Computer Engineering, Ajou University, Suwon, Korea

H. Choo is with the School of Electronic and Electrical Engineering, Hongik University, Seoul, Korea

Color versions of one or more of the figures in this communication are available online at http://ieeexplore.ieee.org.

Digital Object Identifier 10.1109/TAP.2009.2028707

## II. Structure and Characteristics of the Antenna

### A. Single-Layered CP Tag Antenna

If we assume that the reader antenna has ideal RHCP radiation ($\mathrm{AR} \cong 1$), then the backscattering from the tag is normally divided into a structural mode and an antenna mode [6]–[9]. The structural mode is primarily generated by scattering from the external surfaces of the antenna body, ground plate, and substrate materials, so that the polarization of the scattered wave is reversed and becomes LHCP. In contrast, the antenna mode is mainly generated by resonance at the radiator (e.g., microstrip patches and radiating wires), and thus the polarization of the scattered wave is the same as that of the radiator. To prove this, we examined the AR response of the structural and antenna modes separately. The structural mode was obtained from the backscattered field when the tag antenna was fully matched to the tag chip. Then, the antenna mode was calculated by subtracting the structural mode from the backscattering of the shorted tag antenna [10], [11]. As expected, the structural mode showed reversed polarization (close to $\mathrm{AR} = -1$), while the antenna mode showed the same polarization (close to $\mathrm{AR} = 1$) with the incident field. Some researchers have claimed that the reversed polarization of the backscattered signal from the tag would degrade the reading performance at the reader antenna due to the polarization mismatch. However, we found that most of the modulated signal from the tag chip is loaded in antenna mode rather than in structural mode. Thus, the reading range is chiefly determined by backscattered signal in antenna mode. In theory, if the polarization of the tag antenna is matched to that of the reader antenna with CP radiation, the reading range can be twice that possible using a LP tag antenna with the same CP reader antenna.

In this communication, we propose a novel tag antenna capable of greatly increasing the reading range by using CP radiation in a broad bandwidth. Fig. 1 depicts the proposed single-layered tag antenna with RHCP radiation. It consists of a single radiating patch, a shorting plate, a feed line, and a ground plane. The radiating patch is printed on an FR-4 substrate ($\varepsilon_r = 4.2, \tan\delta = 0.02$), and its lower left and upper right corners are truncated by $a \times b$ and $c \times d$ to obtain RHCP radiation [12]. The feed line $d_{\mathrm{feed}}$ is inserted to produce the inductance needed to cancel out the capacitance of the commercial tag chip, and the tag chip is placed at the middle of the feed line [13], [14]. An air substrate is inserted between the FR-4 substrate and the ground plane to broaden the matching bandwidth and reduce the substrate loss [12]. The patch and the ground plane are electrically connected through the feed line and the shorting plate. The shorting plate is bent by $w_{\mathrm{short}} \times \ell_{\mathrm{short}}$ to tune the input impedance by controlling the parasitic capacitance between the patch and the shorting plate. The size of the ground ($w_{\mathrm{GND}} \times \ell_{\mathrm{GND}}$) is limited to less than 150 mm × 150 mm, and the height ($h$) to less than 30 mm, for ease of installation on the target object. The dimensions of the patch are roughly $0.5 \times 0.5\ \lambda$, to resonate at 910 MHz, and the truncated corner is approximately $0.1\ \lambda$, to obtain RHCP operation. The length of the feeding line $d_{\mathrm{feed}}$ is about $0.1\ \lambda$, to produce the required inductance for conjugate matching with the commercial tag chip, which has an input impedance of 20–j 150 [15].

We used the Pareto genetic algorithm (PGA), in conjunction with a FEKO EM simulator, to optimize the design parameters [16], [17]. The rough dimensions listed above were used as the initial values of the design parameters in the PGA process. The design goals were broad matching bandwidth and high AR for CP operation, and hence two cost functions (for attaining these goals) were defined as follows:

$$\mathrm{cost1} = 1 - \sum_{i=1}^{N} \frac{(Z_{\mathrm{in}}(f_i) - Z^*_{\mathrm{chip}}(f_i))/(Z_{\mathrm{in}}(f_i) + Z_{\mathrm{chip}}(f_i))}{N} \times (860\ \mathrm{MHz} < f_i < 960\ \mathrm{MHz}) \quad (1)$$

$$\mathrm{cost2} = \sum_{i=1}^{N} \frac{\mathrm{AR}(f_i)}{N} \quad (2)$$

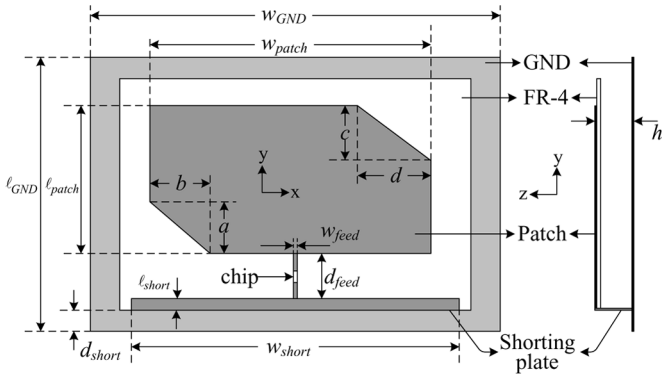


Fig. 1. Structure and design parameters of the proposed single-layered tag antenna to achieve RHCP operation.

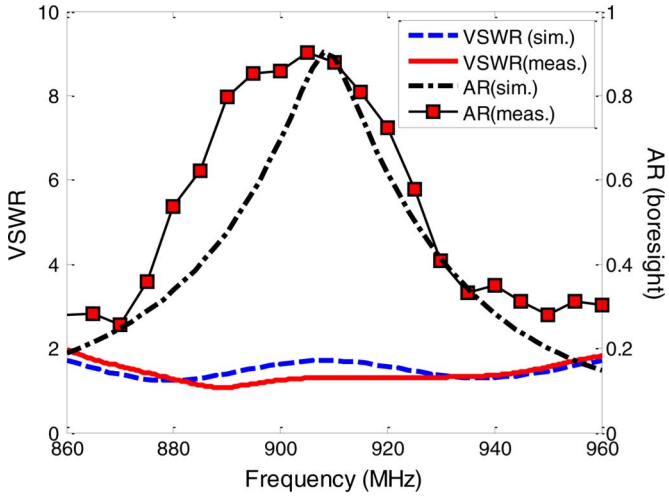


Fig. 2. VSWR and AR of the proposed single-layered tag antenna.

where cost1 is for conjugate matching between the tag chip and the antenna, and cost2, calculated using AR at the boresight ($\theta = 0^\circ$), is used for polarization matching between the tag and reader antennas. The optimized design parameters after 300 iterations of the PGA process are: $a = 40.9$ mm, $b = 8.7$ mm, $c = 32.9$ mm, $d = 43.3$ mm, $w_{\mathrm{feed}} = 2$ mm, $d_{\mathrm{feed}} = 12.4$ mm, $d_{\mathrm{short}} = 4.1$ mm, $w_{\mathrm{patch}} = 136.4$ mm, $\ell_{\mathrm{patch}} = 62.7$ mm, $w_{\mathrm{short}} = 134.2$ mm, $\ell_{\mathrm{short}} = 3.7$ mm, $w_{\mathrm{GND}} = 189.6$ mm, $\ell_{\mathrm{GND}} = 127.9$ mm, and $h = 21.6$ mm.

Fig. 2 shows VSWR and AR (boresight) of the proposed single-layered CP tag antenna. The measured and simulated VSWR are represented by the solid and dashed lines, respectively. The measurements are in fairly close agreement with the simulation results. The double resonances at 890 MHz and 940 MHz induce a broad bandwidth ($\mathrm{VSWR} < 2$), covering the entire UHF RFID band from 860 MHz to 960 MHz. The measured (square mark) and simulated (dash-dot) AR are plotted on a linear scale from $-1$ (LHCP) to 1 (RHCP). Although slight differences exist between the measurements and the simulation results (due to blockage by an additional balun inserted for balanced port measurement), a high AR (close to 1) in the vicinity of 910 MHz is clearly indicated. The bandwidth of the AR ($< 0.707, 3$ dB) is about 15 MHz by simulation, which is much smaller than the impedance bandwidth of about 100 MHz. The narrow AR bandwidth may decrease the reading range, as the frequency used is offset from the center frequency (see the result in Fig. 9).

The reading range of the proposed single-layered tag antenna was measured in response to LP, RHCP, and LHCP reader antennas, and the results are plotted in Fig. 3. The dashed line and the triangular marks represent the simulated and measured reading ranges with a LP reader

TABLE I
PARAMETER VALUES FOR THE READING RANGE AT 912 MHZ

| Parameters | $P_t$ | $G_{reader}$ | $P_{system}$ | $\lambda$ | $G_{tag}$ ($\theta = 0°$) | p ($\theta = 0°$) | | |
|---|---|---|---|---|---|---|---|---|
| | | | | | | with RHCP reader | with LHCP reader | with LP reader |
| values | 1 W | 6 dBi or 6 dBic | – 85 dBm | 0.323 m | 6 dBic | 0.99 | 0.003 | 0.56 |

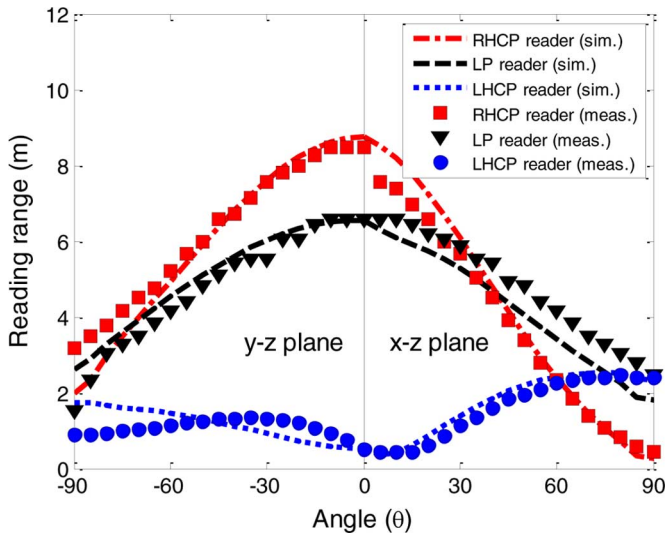


Fig. 3. Reading range of the proposed single-layered tag antenna with RHCP, LP, and LHCP reader antennas.

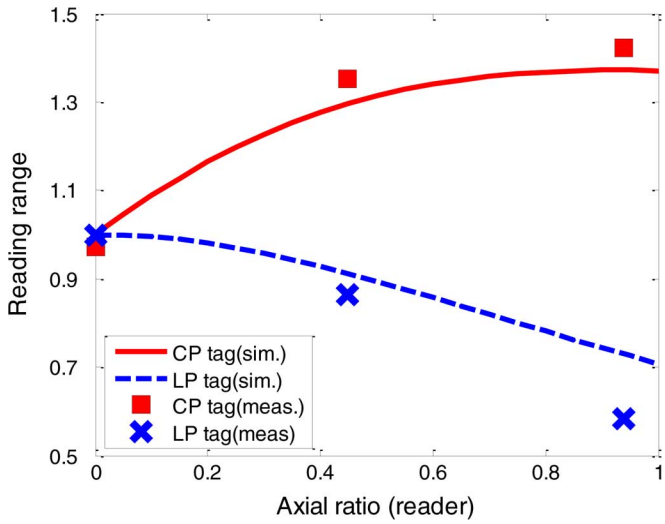


Fig. 4. Reading range as a function of the AR of the reader antenna.

antenna of 6 dBi. Measurements were performed using a TESCOM TC2600A commercial RFID system in an anechoic chamber [18]. The simulations were carried out in accordance with the following:

$$R_{\max} = \sqrt[4]{\frac{P_t G_{\text{tag}}^2 G_{\text{reader}}^2 p^2}{P_{\text{system}}} \left(\frac{\lambda}{4\pi}\right)^4} \tag{3}$$

where $p$ is the polarization efficiency, $G_{\text{tag}}$ is the realized gain of the tag antenna (including the mismatch between the tag antenna and the tag chip), $G_{\text{reader}}$ is the gain of the reader antenna, and $P_{\text{system}}$ is the sensitivity of the reader system in detecting the backscattered signal from the tag. Table I lists all the parameter values used for finding the reading range of the proposed antenna in Fig. 1. The simulated and measured results are in close agreement. The reading ranges of the x-z plane ($\phi = 0^\circ$) and the y-z plane ($\phi = 90^\circ$) are shown on the right and left sides of Fig. 3, respectively. At $\theta = 0^\circ$, the reading ranges are virtually identical, which confirms that the proposed tag antenna attains CP radiation characteristics in the boresight direction ($\theta = 0^\circ$).

The dash-dotted line and the square marks show the simulated and measured reading ranges with an RHCP reader antenna having 6 dBic gain. The reading range using the RHCP reader antenna can be increased by about 40% compared to the LP reader in the region where the AR of the tag is less than 3 dB (x-z plane of about 60° and y-z plane of about 120°). The corresponding results using a LHCP reader are represented by the dotted line (simulation) and the round marks (measurement). With the RHCP reader antenna, the reading range reaches a maximum of about 8 m, while the LHCP reader reduces the reading range to less than 1 m. These results clearly show that the CP tag antenna is capable of increasing the reading range when its polarization is matched with that of the reader antenna. Once again, this occurs because in antenna mode (where the most of the modulated signal is loaded), polarization is not reversed by backscattering.

### B. Characteristics of the CP Tag Antenna

We now turn to a discussion on how the reading range is increased by CP operations. To obtain a clear comparison of CP and LP tags, their reading ranges are normalized and plotted in Fig. 4. All the results are normalized to a fixed reading range of 6.5 m that was measured using the LP tag and the LP reader antenna. The respective simulation and measurement results for the CP tag are depicted by a solid line and square marks, while the corresponding results for the LP tag are represented by a dashed line and 'x' marks. The CP and LP tags perform similarly when they are detected by a LP reader. However, if the AR of the reader is changed from 0 (LP) to 1 (RHCP), the reading range of the CP tag is increased by a factor of 1.4, since the polarization efficiency $p$ is increased from 50% to 100% [19]. For the same reason, the value of $p$ between the LP tag and RHCP reader is reduced by 50%, resulting in a reduced reading range of 0.7 m. Thus, the CP tag is capable of attaining double the reading range of a LP tag, although both have similar reading ranges to the LP reader. In the depolarized environment, the reading range of the CP tag may not simply be doubled, due to the reduced polarization efficiency. However, in many practical situations, such as indoor laboratories, offices, and warehouses, the CP tag shows

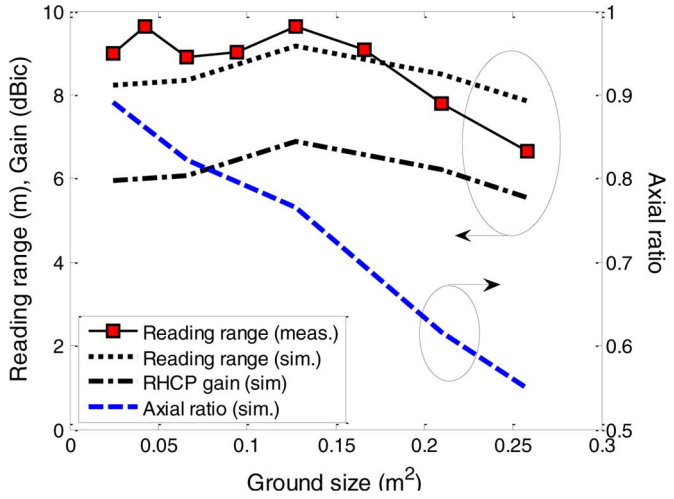


Fig. 5. Reading range and gain as a function of the ground size of the single-layered tag antenna.

better reading range than the LP tag because the depolarization effect exists, but is not that severe.

Fig. 5 shows how the reading range is influenced by other factors. The square marks, dotted line, dashed line, and dash-dotted line represent the measured reading range, simulated reading range, simulated AR of the total scattered field (antenna mode + structural mode), and simulated RHCP gain, respectively. As the ground size increases, scattering in structural mode (LHCP gain) also increases, while scattering in antenna mode (RHCP gain) remains more or less constant, so that the AR of the tag is reduced from 0.9 to 0.55. Since most of the modulated signal is loaded in antenna mode (RHCP gain) rather than structural mode (LHCP gain), the reading range of the tag remains nearly unchanged. In addition, the graphical shape of the simulated RHCP gain is very similar to that of the simulated reading range. The trend of the measured results clearly shows the close relationship between the RHCP gain and the reading range. Therefore, to enlarge the reading range, the antenna should be optimized for high RHCP gain. In the next section, we describe a double-layered tag antenna capable of accomplishing this.

### C. A Double-Layered Tag Antenna for Broad Bandwidth Operation

To widen the frequency band in which the reading range exceeds 6 m, we propose the use of a double-layered tag antenna capable of attaining high RHCP gain over a broad bandwidth. The antenna has an additional parasitic patch located at a height $h_2$ above the single-layered tag antenna, as shown in Fig. 6, [20]–[22]. The parasitic patch is printed on the FR-4 substrate, and again the edge of the patch is truncated by $a_2 \times b_2$ and $c_2 \times d_2$ to obtain RHCP radiation. In addition, to reduce the ground size while maintaining antenna performance, the edge of the ground is folded upward to a height $h$. The design parameters are again optimized via PGA using the following two cost functions:

$$\text{cost1} = 1 - \sum_{i=1}^{N} \frac{\text{Gain}_{\text{RHCP}}(f_i)}{N} \times (860\,\text{MHz} < f_i < 960\,\text{MHz}) \quad (4)$$

$$\text{cost2} = \text{size}. \quad (5)$$

As discussed in the previous section, the reading range of the tag is dependent on RHCP gain, rather than AR. Thus, cost1 is now adapted to optimize the bandwidth of RHCP gain ($> 5$ dBic), and cost2 is applied to the GA for the reduction of the antenna size. Fig. 7 shows the optimized results for the single- and double-layered tag antennas, represented by the square and triangular marks, respectively. As we increase the ground size, the bandwidth of RHCP gain also increases. Under the same conditions, the double-layered tag antenna attains a

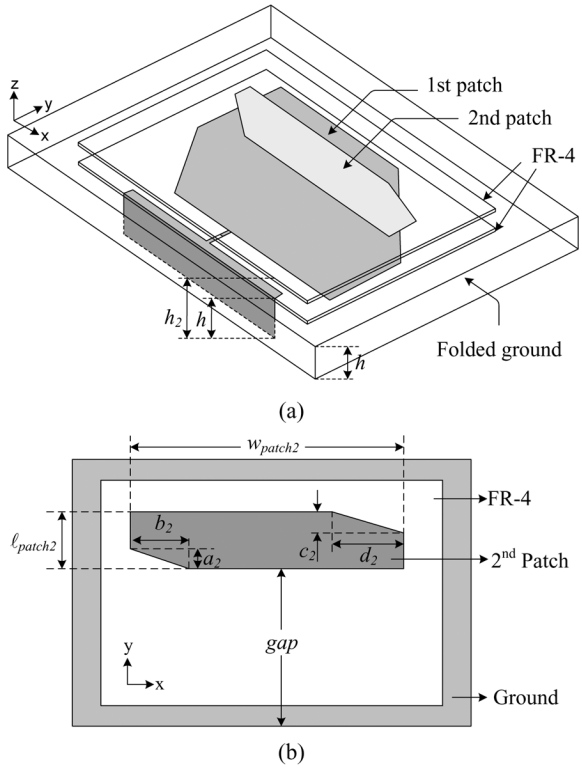


Fig. 6. Structure and design parameters of the proposed double-layered tag antenna to operate in the worldwide UHF RFID band (a) perspective drawing (b) layout of the second patch.

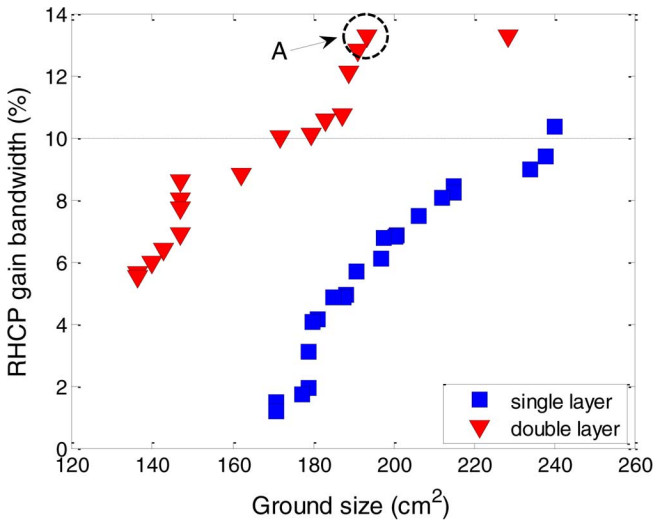


Fig. 7. Optimized results for the single- and double-layered tag antennas.

bandwidth nearly twice that of the single-layered tag antenna. This result demonstrates that the bandwidth of RHCP gain is broadened by loading the parasitic patch. To attain a bandwidth covering the entire UHF RFID band, the single-layered tag antenna requires a ground size larger than 240 cm$^2$, whereas for the double-layered tag, a ground size of only 170 cm$^2$ is sufficient.

To confirm the optimized results, we built a sample antenna, denoted by 'A' in Fig. 7. Its design parameters were as follows: $a = 39.3$ mm, $b = 13.2$ mm, $c = 77.2$ mm, $d = 57.0$ mm, $w_{\text{feed}} = 2$ mm, $d_{\text{feed}} = 13.1$ mm, $d_{\text{short}} = 3.8$ mm, $w_{\text{patch}} = 138.2$ mm, $\ell_{\text{patch}} = 88.4$ mm, $w_{\text{short}} = 104.2$ mm, $\ell_{\text{short}} = 4.7$ mm, $w_{\text{GND}} = 158.6$ mm, $\ell_{\text{GND}} = 122.0$ mm, $h = 11.9$ mm, $a_2 = 8.7$ mm, $b_2 = 23.6$ mm, $c_2 =$

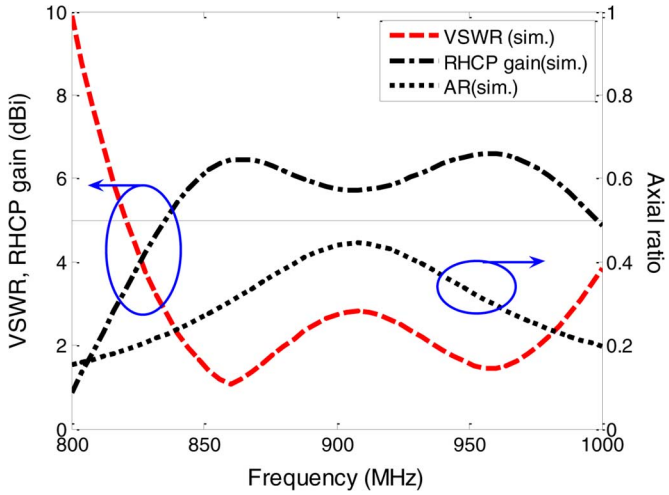


Fig. 8. VSWR, RHCP gain, and AR of the double-layered antenna.

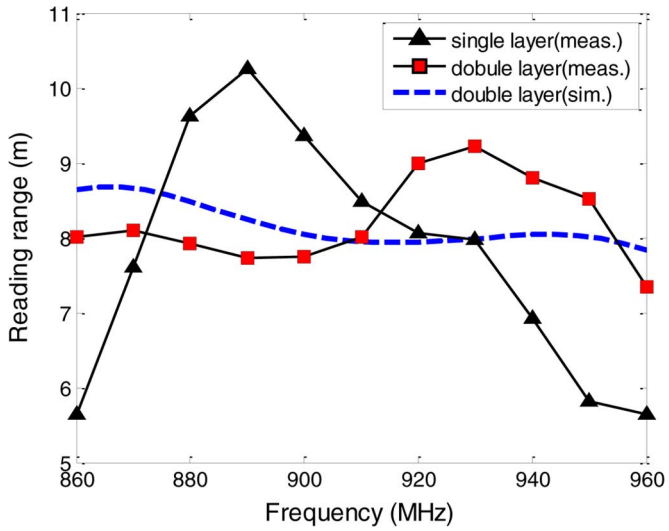


Fig. 9. Reading range as a function of operating frequency.

7.4 mm, $d_2 = 56.0$ mm, $w_{\mathrm{patch2}} = 123.8$ mm, $\ell_{\mathrm{patch2}} = 11.7$ mm, $h_2 = 30.6$ mm, and gap $= 75.9$ mm. Fig. 8 shows VSWR (dashed line), RHCP gain (dash-dotted line), and AR (dotted line) for sample A. The sample antenna exhibits low VSWR over a wide frequency range. Although the sample antenna has a low AR (only 0.45) at the central frequency of 910 MHz, it has high RHCP gain ($> 5$ dBic) over a wide range of frequencies, and its reading range exceeds 6 m from 860 MHz to 960 MHz. To verify this result, we measured the reading ranges of the single- and double-layered tag antennas at various frequencies. In Fig. 9, the measured and simulated reading ranges of the double-layered tag are represented by the square marks and the dashed line, respectively. The measured results differ little (by less than 1 m) from the simulated results, since we assume that the input impedance of the tag chip is constant with respect to frequency (although the exact value of the impedance is affected by frequency). The reading range of the single-layered tag (triangular marks) is also plotted in Fig. 9 for the sake of comparison. The reading range of the double-layered tag antenna is 8 m at 860 MHz compared to 5.5 m for the single-layered tag antenna, and 7.5 m at 960 MHz compared to 5.5 m for the single-layered tag antenna. This result indicates that the single-layered tag can be more attractive than the double-layered tag for narrowband applications, but to be used in worldwide applications, the double-layered tag antenna with broad RHCP gain bandwidth may be a more suitable solution.

## III. Conclusion

In this communication, we introduced an innovative tag antenna capable of greatly increasing RFID reading range by using CP radiation. The proposed antenna consists of a single radiating patch, a shorting plate, and a ground plane. Detailed design parameters were optimized using PGA in conjunction with the FEKO EM simulator. The measured impedance bandwidth entirely covers the UHF RFID band, and a high AR (close to 1) is obtained near 910 MHz. The reading range was measured with a commercial RIFD system, and the reading range of the CP tag was confirmed to be capable of attaining twice that of the LP tag. We also found that the reading range is primarily determined by the RHCP gain of the tag antenna rather than the AR. Finally, to increase the RHCP gain over a wide band of frequencies, we modified the antenna structure by loading an additional parasitic patch on top of it. The double-layered tag achieves twice the RHCP gain bandwidth of the single-layered tag, and has a reading range of about 8 m from 860 MHz to 960 MHz.

## References

[1] D. Brown, *RFID Implementation*. New York: McGraw-Hill, 2007.
[2] C. Floerkemeier, C. Roduner, and M. Lampe, "RFID application development with the Accada middleware platform," *IEEE Syst. J.*, vol. 1, no. 2, pp. 82–94, Dec. 2007.
[3] R. Weinstein, "RFID: A technical overview and its application to the enterprise," *IT Professional*, vol. 7, no. 3, pp. 27–33, May–Jun. 2005.
[4] K. Finkenzeller, *RFID Handbook*, 2nd ed. West Sussex, U.K.: Wiley, 2003.
[5] *Regulatory Status for Using RFID in the UHF Spectrum*, , Jan. 20, 2008 [Online]. Available: www.epcglobalinc.org
[6] K. Penttila, M. Keskilammi, L. Sydanheimo, and M. Kivikoski, "Radar cross-section analysis for passive RFID systems," *IEE Proc. Microw. Antennas Propag.*, vol. 153, no. 1, pp. 103–109, Feb. 2006.
[7] P. V. Nikitin and K. V. S. Rao, "Theory and measurement of backscattering from RFID tags," *IEEE Antennas Propag. Mag.*, vol. 48, no. 6, pp. 212–218, Dec. 2006.
[8] S. Hu, C. L. Law, and W. Dou, "A balloon-shaped monopole antenna for passive UWB-RFID tag applications," *IEEE Antennas Wireless Propag. Lett.*, vol. 7, pp. 366–368, 2008.
[9] L. Sydanheimol, J. Nummetla, L. Ukkonen, J. McVay, A. Hoorfar, and M. Kivikoskil, "Characterization of passive UHF RFID tag performance," *IEEE Antennas Propag., Mag.*, vol. 50, no. 3, pp. 207–212, Jun. 2008.
[10] W. L. Stutzman and G. A. Thiele, *Antenna Theory and Design*, 2nd ed. New York: Wiley, 1998.
[11] C. A. Balanis, *Antenna Theory: Analysis and Design*, 2nd ed. New York: Wiley, 1997.
[12] R. Garg, P. Bhartia, I. Bahl, and A. Ittipiboon, *Microstrip Antenna Design Handbook*. Norwood, MA: Artech House, 2001.
[13] P. V. Nikitin, K. V. S. Rao, S. F. Lam, V. Pillai, R. Martinez, and H. Heinrich, "Power reflection coefficient analysis for complex impedances in RFID tag design," *IEEE Trans. Microw. Theory Tech.*, vol. 53, no. 9, pp. 2721–2725, Sep. 2005.
[14] C. Cho, H. Choo, and I. Park, "Design of planar RFID tag antenna for metallic objects," *Electron. Lett.*, vol. 44, no. 3, pp. 175–177, Jan. 2008.
[15] Impinj RFID Chips [Online]. Available: www.impinj.com
[16] H. Choo, R. Rogers, and H. Ling, "Design of electrically small wire antennas using a pareto genetic algorithm," *IEEE Trans. Antennas Propag.*, vol. 53, no. 3, pp. 1038–1046, Mar. 2005.
[17] FEKO Suite 5.3. [Online]. Available: www.feko.info
[18] TC-2600A RFID Tester [Online]. Available: www.tescom.co.kr
[19] W. Stutzman, *Polarization in Electromagnetic Syst.*. Norwood, MA: Artech House, 1993.
[20] N. Herscovici, Z. Sipus, and D. Bonefacic, "Circularly polarized single-fed wide-band microstrip patch," *IEEE Trans. Antennas Propag.*, vol. 51, no. 6, pp. 1277–1280, Jun. 2003.
[21] K. L. Chung and A. S. Mohan, "A systematic design method to obtain broadband characteristics for singly-fed electromagnetically coupled patch antennas for circular polarization," *IEEE Trans. Antennas Propag.*, vol. 51, no. 12, pp. 3239–3248, Dec. 2003.
[22] Nasimuddin, K. P. Esselle, and A. K. Verma, "Wideband circularly polarized stacked microstrip antennas," *IEEE Antennas Wireless Propag. Lett.*, vol. 6, pp. 21–24, 2007.